World Journal of Advanced Research and Reviews
eISSN: 2581-9615 CODEN (USA): WJARAI
Cross Ref DOI: 10.30574/wjarr
Journal homepage: https://wjarr.com/

(RESEARCH ARTICLE)

Check for updates

Investigation of the corrosion inhibition potential of *Axonopus compressus* (Carpet grass) Extract on Mild steel in $C0_2$corrosive media

Olusegun Peter Akinyemi [1,*], Favour Oluwadarasimi Emmanuel [1], Oghenemetega Divine Edoja [1] and David Asuquo Ante [2]

[1] *Department of Chemical Engineering, Faculty of Engineering, Lagos State University, Ojo, Nigeria.*
[2] *Department of Chemistry, Louisiana State University, USA.*

World Journal of Advanced Research and Reviews, 2025, 27(02), 741-754

Publication history: Received on 17 June 2025; revised on 22 July 2025; accepted on 25 July 2025

Article DOI: https://doi.org/10.30574/wjarr.2025.27.2.2640

Abstract

Corrosion remains a formidable challenge in process plants, necessitating eco-friendly mitigation strategies. This study explores the potential of *Axonopus compressus* (Carpet grass) extract as a corrosion inhibitor for mild steel in a CO_2 saline environment.

The aim is to advance the understanding of environmentally friendly corrosion inhibitors in a CO_2 saline environment, containing 3.5% NaCl. The project's objectives encompass phytochemical extraction, characterization, and corrosion inhibition potential evaluation. The extraction of *Axonopus compressus* was conducted through the solvent extraction method employing methanol. Various concentrations of the extract were subjected to testing within a temperature of 30°C and 60°C, pH of 6.0, and for an immersion period of 163 hours. The corrosion inhibition assessment utilized the gravimetric (Weight Loss) method.

The results of the experiments revealed a remarkable corrosion inhibition efficiency of 93% at a temperature of 30°C and concentration of 2.8g in 100ml of solution for the *Axonopus compressus* extract. At 60°C, the corrosion rate was found to increase significantly, and the inhibition efficiency decreased slightly, particularly at lower concentrations, though high concentrations still maintained substantial protective effects. Notably, the inhibition efficiency exhibited a positive correlation with the concentration of the extract. As the concentration increased, the inhibitive effect on corrosion demonstrated a corresponding enhancement. The adsorption isotherm for the adsorption of *Axonopus compressus* extract on the steel surface was found to follow the Langmuir adsorption isotherm.

Keywords: Green corrosion inhibition; *Axonopus compressus* Extract;$\boldsymbol{CO_2}$ saline environment; Mild Steel; Langmuir Adsorption Isotherm

1. Introduction

Corrosion is a term that describes the transformation of pure metals and their alloys to a more stable thermodynamic state as a result of a reaction with their surroundings, and this stable state may include their various sulfides, hydroxides, and oxides. The effect of corrosion on properties is quitea lot as they may cause damage like leakages, facility downtime, and collapse of a system which can be injurious and hazardous [1]. The fundamental element that drives corrosion is the potential energy difference between the potential energy of the corroding metal and the corrosion product. In the extraction of metals from their ores, there is a required amount of energy used to achieve this and after a while, this metal finds a way of returning to its original energy level when it finally begins to interact with its environment [2].

*Corresponding author: Olusegun Peters Akinyemi

$C0_2$corrosion,also referred to as sweet corrosion, is commonly associated with mild steel and represents a significant challenge within various production sectors, notably in the oil and gas industry, where the presence of both water and oil is prevalent [3].

The presence of acidic gases such as $C0_2$ and H_2S in produced fluids aggravates corrosion tendencies in production facilities and can cause localized or pitting corrosion in steels [4]. The emergence of the use of CO_2 injection for enhanced oil recovery makes CO_2 corrosive media a common issue in the exploration of gas reservoirs [5]. CO_2 is soluble in the formation water that comes to the surface with production fluid and eventually forms a weak carbonic acid (H_2CO_3) which is extremely corrosive to carbon steel. F_eCO_3 is believed to be the main corrosion product formed with carbon steel in a corrosive media and some cathodic mechanisms have been proposed to soothe the CO_2 corrosion behavior with CO_2 believed to accelerate the cathodic reaction [6].

1.1. $C0_2$ Corrosion Mechanism on Mild Steel

$\boldsymbol{C0_2}$corrosionis a significant concern in industries like oil and gas, where mild steel is commonly used due to its cost-effectiveness and strength. The corrosion process involves several key steps:

The process begins with the dissolution of carbon dioxide $\boldsymbol{C0_2}$in water ($\boldsymbol{H_2O_{(l)}}$) that accompanies production fluids. $\boldsymbol{C0_2}$, a gas, is highly soluble in water, leading to its conversion into aqueous $\boldsymbol{C0_{2\,(aq)}}$ [7].

$$\boldsymbol{C0_{2\,(g)} \rightleftharpoons C0_{2\,(aq)}} \quad \ldots\ldots\ldots\ldots\ldots\ldots (1)$$

$C0_{2\,(aq)}$ reacts with water to form carbonic acid (H_2CO_3). This reaction occurs due to the interaction between $\boldsymbol{C0_2}$ molecules and water molecules. According to a study by Nešić [8], as cited in the study by Fazal [6],only a minor portion, approximately 0.2%of the dissolved CO_2 reacts with water to form carbonic acid. The reaction is described by (Eq 1) and (Eq 2), respectively.

$$\boldsymbol{C0_{2\,(aq)} + H_2O_{(l)} \rightleftharpoons H_2CO_3} \ldots\ldots\ldots\ldots\ldots\ldots\ldots (2)$$

Carbonic acid is a weak acid but is corrosive to mild steel because it initiates the corrosion process.

Carbonic acid undergoes dissociation into hydrogen ions (H^+) and bicarbonate ions (HCO_3^-) in an equilibrium reaction:

$$\boldsymbol{H_2CO_3 \rightleftharpoons H^+ + HCO_3^-} \ldots\ldots\ldots\ldots\ldots\ldots\ldots (3)$$

The presence of hydrogen ions is a critical factor in the corrosion process.

Cathodic Reaction: Reduction of Protons: One of the primary cathodic reactions involves the reduction of protons H^+

$$\boldsymbol{2H^+ + 2e^- \rightleftharpoons H_2} \quad \ldots\ldots\ldots\ldots\ldots\ldots\ldots (4)$$

This reduction reaction produces hydrogen gas (H_2) as a byproduct.

While the reduction of protons is commonly accepted as the main cathodic reaction as in (Eq 5), a proposed 'buffer effect mechanism' suggests that the equilibrium reaction of carbonic acid primarily serves to supply more hydrogen ions (H^+) rather than directly participating in the reduction process [6, 9].

$$\boldsymbol{H_2CO_3 + 2e^- \rightleftharpoons HCO_3^- + H_2} \quad \ldots\ldots\ldots\ldots\ldots\ldots\ldots (5)$$

This mechanism posits that the primary reduction occurs with protons (H^+).

Role of Temperature: It's important to note that the rate-controlling step for cathodic reaction kinetics is often the hydration of carbon dioxide ($C0_{2\,(g)}$) to carbonic acid (H_2CO_3), especially at temperatures below 50–60 °C [8].

Anodic Reaction - Iron Dissolution: To balance the cathodic reactions, mild steel (iron) undergoes anodic dissolution:

$$\boldsymbol{Fe_{(s)} \rightarrow Fe_2^+ + 2e^-} \quad \ldots\ldots\ldots\ldots\ldots\ldots\ldots (6)$$

The dissolved iron ions enter the solution as part of the corrosion process.

Adsorption and Oxidation of Iron Ions: Iron combines with water (H_2O) to form adsorbed intermediate products:

$$Fe_{(s)} + OH^- \rightarrow FeOH + e^- \text{ (adsorption)} \quad \ldots\ldots\ldots\ldots\ldots\ldots\ldots (7)$$

The adsorbed intermediate products then oxidize further:

$$FeOH \rightarrow FeOH_2^+ + e^- \quad \ldots\ldots\ldots\ldots\ldots\ldots\ldots (8)$$

These reactions contribute to the overall anodic dissolution of iron.

For the case of mild steel one can write the overall reaction as;

$$Fe_{(s)} + CO_2 + H_2O \rightarrow Fe_2^+ + CO_3^{2-} + H_2 \quad \ldots\ldots\ldots\ldots\ldots\ldots\ldots (9)$$

In essence, $C0_2$ corrosion on mild steel is a complex electrochemical process involving the dissolution of $C0_{2\,(g)}$ in water, the formation of carbonic acid, the reduction of protons, and the anodic dissolution of iron [10]. The specific reactions can vary depending on factors such as temperature, pH, and the presence of inhibitors [11].

1.2. Green Corrosion Inhibitors

Green Corrosion Inhibitors can be natural or synthetic, as seen in figure 1. The idea of the use of plants has been recognized as a potential replacement for organic compounds and there have been numerous research in the last decade and more to be done in years to come, it is believed that the use of naturally occurring compounds is of interest because of their cost-effectiveness, easy accessibility of raw materials and eco-friendliness. When selecting an inhibitor, several factors merit consideration, including the inhibitor's cost, potential toxicity impacting humans and other living organisms, its availability, and its environmental friendliness [12]. Plant extracts serve as viable options for environmentally friendly alternatives [13]. According to Sapunyo W.L. [14], the aqueous methanol, and dichloromethane: methanol (1:1) extracts of *Axonopus compressus* (carpet grass) possess phytochemical compounds with anticandidal activity. The extracts have also been classified as non-toxic [14].

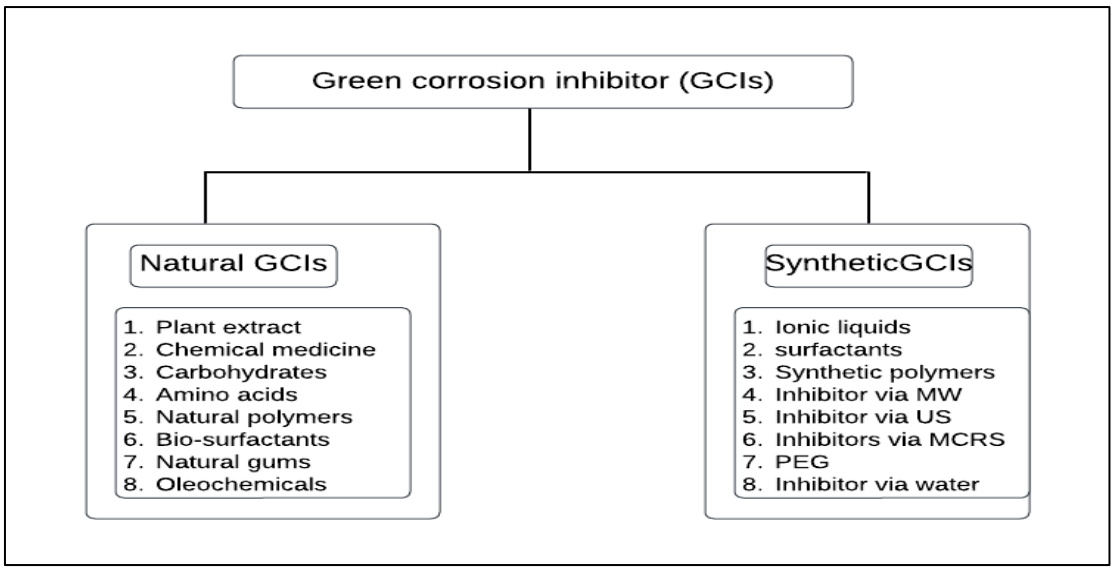

Figure 1 Natural and Synthetic green corrosion inhibitor

Given the growing environmental and economic concerns surrounding corrosion, especially in CO_2-rich saline environments such as oil and gas pipelines and process plants, there is an increasing need for eco-friendly corrosion mitigation strategies. Conventional inhibitors are often synthetic and toxic, posing environmental and safety risks. As a result, attention has shifted towards plant-based green inhibitors that are biodegradable, cost-effective, and sustainable.

This study explores *Axonopus compressus* as a novel green corrosion inhibitor for mild steel in a CO_2-saturated 3.5% NaCl medium. The aim is to advance the understanding of the inhibition mechanism of this plant extract by evaluating its phytochemical composition, adsorption behaviour, and inhibition performance under different environmental conditions.

2. Materials and Methods

2.1. Preparation of Carpet grass extract

Axonopus compressus, sourced from the vicinity of Epe in Lagos, Nigeria, underwent a series of preparation steps. Initially, it was subjected to washing and subsequent air-drying. Following this, it was exposed to an oven set at 45°C where it remained for 48 hours. The resulting dried carpet grass was then processed into a powdered form using a miller. To achieve a finer consistency, the powder was sieved through a mesh with a size of 10mm. Finally, the fine particles were carefully stored in an airtight container and placed inside a desicator for safekeeping.

Cold extraction was used. A quantity of one hundred grams (100g) of the milled carpet grass was measured in 100% methanol for 48 hours, shaking sporadically every two hours. After filtering the extract through Whatman filter sheets No. 42 (125 mm), the solvent was recovered using steam distillation with the water bath set at 70^oC and the resulting wet residue was dried in an electric oven set at 40^oC. The crude extract was stored in sealed plastic container at 4 °C in a refrigerator until when needed. Using the following formula, the extract's percentage yield was determined.

$$\text{Ratio for Cold Maceration} = \frac{Mass\ of\ carpet\ grass}{Volume\ of\ Solvent} \quad \ldots\ldots\ldots\ldots\ldots\ldots \quad (10)$$

$$\text{Ratio of Methanol Recovered} = \frac{\text{Volume of Recovered Methanol}}{\text{Volume of solvent used}} \quad \ldots\ldots\ldots\ldots\ldots\ldots \quad (11)$$

$$\text{Yield} = \frac{Mass\ of\ Extract}{Mass\ of\ carpet\ grass} \times 100 \quad \ldots\ldots\ldots\ldots\ldots\ldots \quad (12)$$

2.2. Preparation of Metal Specimen

Mild steel sheets of 1 mm thickness were cut into eleven identical coupons with dimensions of 3 cm × 3 cm × 0.1 cm. To ensure surface cleanliness, each coupon was polished using sandpaper to remove surface oxides and impurities, then rinsed with analytical-grade ethanol. Degreasing was subsequently carried out using acetone to eliminate residual oil or grease that could interfere with surface interactions during testing. One of the coupons was selected and submitted to the Quality Control Laboratory for elemental analysis. The remaining ten coupons were individually labeled and reserved for the corrosion inhibition experiments. Each coupon was weighed using a precision balance (±0.01 g), and the initial weights were found to be approximately 6.43 g, confirming uniformity in dimensions and material density.

Figure2 The Energy Dispersive X-ray Spectroscopy (EDS) shows the elemental analysis of mild steel before corrosion study. The EDS compositional analysis results obtained from the spectra show a weight percent of Carbon (3.0 wt. %), Oxygen (20.0 wt. %), Iron (54.0 wt. %), Aluminum (2.00 wt. %), Magnesium (4.00wt%), Zinc (8.40), Calcium (1.30wt%), Potassium (2.00wt%), Silicon (1.20wt%) and Titanium (4.00wt %) for the mild steel before corrosion experiment.

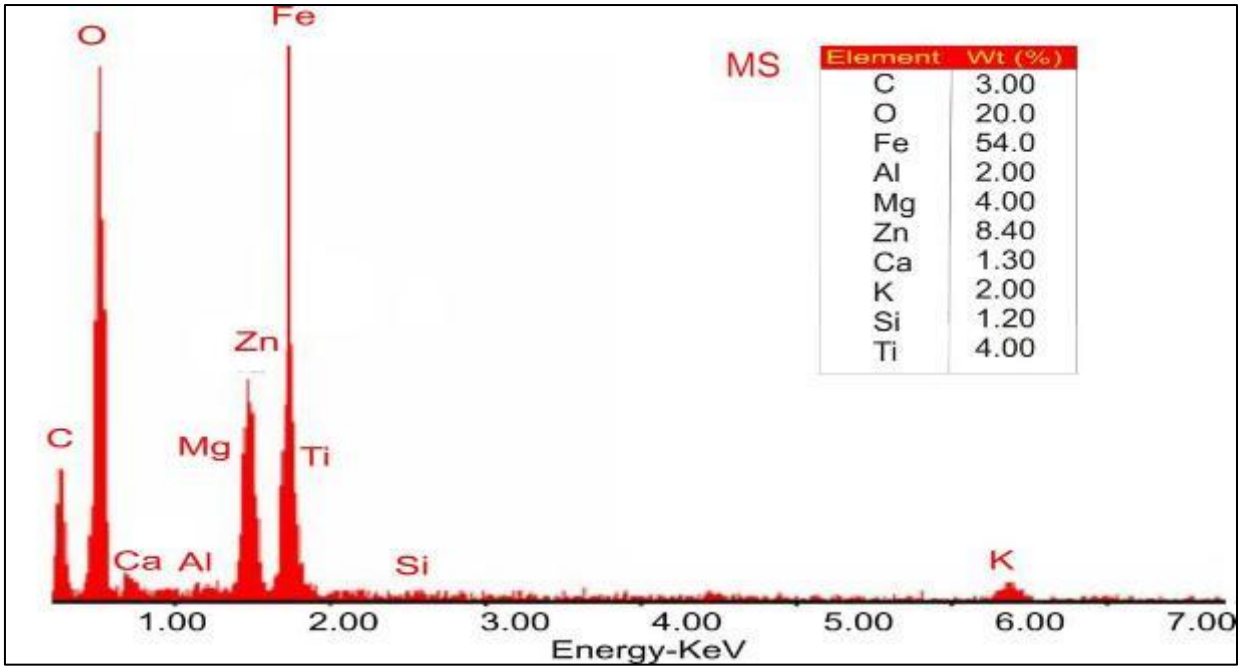

Figure 2 Energy Dispersive X-Ray Spectroscopy Analysis of Mild Steel

After drying the specimens in an oven at 40 °C, their initial weights were re-measured. The volume of the test solution was deliberately kept large enough to ensure the detection of any significant changes in its corrosive properties, whether due to the depletion of active corrosive species or the accumulation of corrosion byproducts. To preserve the prepared mild steel in a dust-free environment, the specimens were stored in desiccators and used immediately for the corrosion experiments after preparation.

2.3. Evaluation of Corrosion inhibition of mild steel (Weight Loss)

CO_2 gas was continuously purged into a sealed bottle containing distilled water for approximately 15 minutes to ensure saturation, as illustrated in Figure 3. Following this, a solution was prepared by combining 100 mL of the CO_2-saturated water with 3.5% NaCl, adjusted to a pH of 6.0. This solution was then evenly distributed into ten separate beakers. Subsequently, varying concentrations (10%, 20%, 30%, and 40%) of the methanolic plant extract (as shown in Figure 3) were added individually to designated beakers. Each beaker received a pre-weighed mild steel coupon, after which all beakers were placed in water baths set at 30 °C and 60 °C, respectively. The immersion process lasted for 163 hours.

After the exposure period, the steel samples were carefully removed, cleaned, dried, and reweighed. The mass loss was recorded meticulously for further analysis of corrosion rates and inhibition efficiency. The weight loss (Δw), corrosion rate (CR), inhibition efficiency (IE) and degree of surface coverage were calculated using standard equations

$$\Delta W = W_i - W_f \quad \text{..... (13)}$$

$$IE\% = \frac{W_0 - W_1}{W_0} \quad \text{..... (14)}$$

$$\theta = \frac{W_0 - W_1}{W_0} \quad \text{..... (15)}$$

$$\text{CR (mmpy)} = \frac{\text{K x Weight loss}}{\text{D x A x t (in hours)}} \quad \text{..... (16)}$$

Figure 3 Photographs showing preparation *of Axonopus compressus* Extract and solution.

Where W_i and W_f are the initial and final weight of mild steel samples respectively; W_1 and W_0 are the weight loss values in presence and absence of inhibitor respectively. A is the area cm^2, t is the time K = $8.76x10^4$ (constant)), D is density in gm/cm^3 (7.86).

3. Result and discussion

3.1. Yield and Characterization of Methanolic Extract

Table 1 Qualitative Phytochemical Analysis of Extract

Plant Phytochemicals	Plant Metabolite
Cardiac glycosides	+++
Steroid glycosides	++
Saponins	+ +
Tannins	++

Alkaloids	+++
Phlobatannins	+
Terpenoids	+
Flavonoids	++
Anthraquinones	+++

-= Absent, + = Present, ++=Moderate, +++ = Abundant

The methanolic leaf extract of *Axonopus compressus* had a greenish color and yielded 7% w/w of the dry matter. The composition of the phytochemical extract is summarized in Table 1.

The phytochemical screening of *Axonopus compressus* indicated the presence of steroids (steroid glycoside), alkaloids, saponins, tannins, cardiac glycosides, flavonoids, phlobatannins, anthraquinones, and terpenes. Quantitative analysis revealed high levels of flavonoids, and alkaloids, along with significant amounts of polyphenolsconsistent with findings reported by Afolabi [15].

3.2. Weight Loss Measurement

Table 2 – Table 3 show the various samples, their respective concentrations, weight loss values, inhibition efficiency (η %) and surface coverage (θ) for mild steel at different concentrations of *Axonopus compressus* extract. These values were calculated after immersion in CO_2 corrosive media. From Table3, the analysis shows that the minimum weight loss was observed when the mild steel samples were immersed in the test solution containing *Axonopus compressus* extract for 163 hours, with concentration ranges from 10% (w/w) to 40% (w/w) at 30°C. In particular, Sample C (40% w/w) exhibited the least weight loss (0.01 g), followed by Sample B (30% w/w) with 0.04 g, indicating effective inhibition at higher concentrations.

Table 2 The labeling of all extract samples and there corresponding concentration(w/v).

Sample	**Concentration (w/v)**	**Percentage (%w/w)**
Sample A (Blank)	0	0
Sample B	2.1	30
Sample C	2.8	40
Sample D	0.7	20
Sample E	0.4	10

Table 3 The data for varying weight of mild steel with different concentration of *Axonopus compressus* extract at the two temperatures studied.

Time (hr.)	**Sample A (g)**		**Sample B (g)**		**Sample C (g)**		**Sample D (g)**		**Sample E (g)**	
	30 ^{0}C	60 ^{0}C	30 ^{0}C	60 ^{0}C	30 ^{0}C	60 ^{0}C	30 ^{0}C	60 ^{0}C	30 ^{0}C	60 ^{0}C
0	6.43	6.43	6.43	6.43	6.43	6.43	6.43	6.43	6.43	6.43
163	6.29	4.68	6.39	5.83	6.42	6.13	6.38	5.68	6.37	5.53

In contrast, the blank sample (Sample A), which had no inhibitor, recorded a weight loss of 0.14 g at 30°C and 1.75 g at 60°C, confirming the absence of any protective barrier against corrosion.

Thus, compared to the result of the blank, i.e., without the presence of inhibitor, it can be observed that the *Axonopus compressus* extract (Inhibitor) caused a reduction in weight loss and consequently reduced the corrosion rate at both 30°C and 60°

From the analysis above, it is evident that the carpet grass extract significantly improved corrosion resistance of mild steel by reducing the weight loss across all concentrations when compared to the blank. The higher the concentration of the extract, the greater the inhibition efficiency, with optimal results seen at 40% and 30% w/w.

3.3. Corrosion Rate

The corrosion rate of mild steel in CO_2-saturated corrosive media was evaluated in the presence and absence of *Axonopus compressus* (carpet grass) extract, and the results are presented in Figure4 and Table 4. It was observed that the corrosion rate decreased with increasing concentration of the extract, indicating the effectiveness of *Axonopus compressus* as a corrosion inhibitor.

At 30°C, the blank sample (Sample A), which contained no inhibitor, exhibited the highest corrosion rate of 9.57 mm/year, while the lowest corrosion rate of 0.68 mm/year was recorded for Sample C (2.8 g/ml or 40% w/w extract concentration). A similar trend was observed at 60°C, where the corrosion rate for the blank rose significantly to 119.66 mm/year, compared to 20.52 mm/year for the same highest concentration of inhibitor. This reduction in corrosion rate is attributed to the adsorption of phytochemical constituents of the carpet grass extract onto the surface of the mild steel, forming a protective barrier that hindered further interaction with the corrosive medium.

Table 4 The Corrosion rate (CR), Inhibition efficiency (IE%) and surface coverage (θ) with different concentration of *Axonopus compressus* extract at the two temperatures studied.

Sample	Conc. (g/ml)	Weight Loss (g)		CR (mmpy)		IE%		(θ)	
		30 ^{0}C	60^{0}C	30^{0}C	60^{0}C	30^{0}C	60^{0}C	30^{0}C	60^{0}C
Sample A	0	0.14	1.75	9.57	119.66	0	0	0	0
Sample E	0.4	0.06	0.9	4.1	61.54	57.14	48.57	0.57	0.49
Sample D	0.7	0.05	0.75	3.42	51.28	64.29	57.14	0.64	0.57
Sample B	2.1	0.04	0.6	2.73	41.02	71.43	65.71	0.71	0.66
Sample C	2.8	0.01	0.3	0.68	20.52	92.86	82.86	0.93	0.83

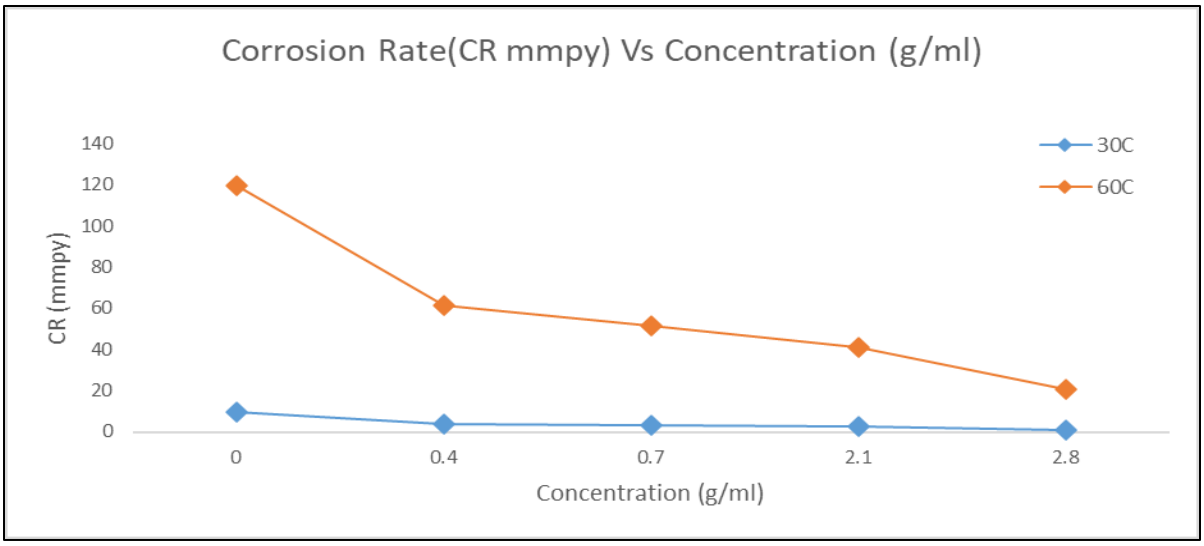

Figure 4 The variation of Corrosion Rate with extract concentration at the two temperatures studied.

3.4. Effects of Concentration on Inhibition Efficiency

The inhibition efficiency of *Axonopus compressus* extract increased progressively with rising inhibitor concentration as shown in Figure 5. This trend was evident at both 30°C and 60°C, indicating that the protective action of the extract on mild steel is strongly dependent on its concentration in the corrosive medium. At 30°C, inhibition efficiency increased from 57.14% at 0.4 g/ml (Sample E) to 92.86% at 2.8 g/ml (Sample C), while at 60°C, a corresponding increase from

48.57% to 82.86% was observed. This steady improvement suggests that more inhibitor molecules are adsorbed onto the steel surface at higher concentrations, thereby enhancing surface coverage and reducing access of the corrosive species to the metal substrate. The slight reduction in inhibition efficiency at elevated temperatures may be attributed to increased desorption of the inhibitor molecules due to thermal agitation, which weakens the integrity of the adsorbed film. Despite this, the extract still retained considerable efficiency, even at 60°C, confirming its potential as a viable green corrosion inhibitor under varying thermal conditions.

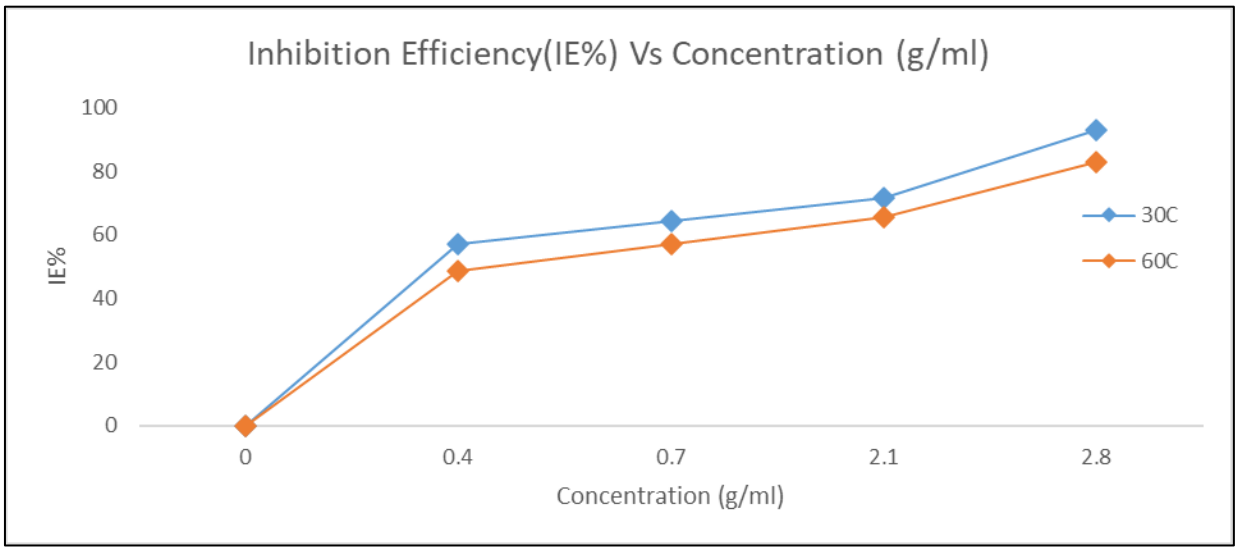

Figure 5 The variation of inhibition efficiency with extract concentration at the two temperatures studied.

3.5 Effects of Surface Coverage (θ)

Surface coverage (θ) is a dimensionless parameter that represents the fraction of the metal surface covered or protected by the inhibitor molecules. It provides insight into the extent of adsorption of the inhibitor onto the metal surface, where a value of 1 indicates complete coverage and 0 implies no adsorption. A higher surface coverage value suggests more effective barrier formation against corrosion [16]. In this study, surface coverage increased with the concentration of *Axonopus compressus* extract, consistent with the observed trends in corrosion rate and inhibition efficiency. At 30°C, θ increased from 0.57 at 0.4 g/ml (Sample E) to 0.93 at 2.8 g/ml (Sample C). A similar increase was recorded at 60°C, where θ rose from 0.49 to 0.83 across the same concentration range.

These results indicate that the extract's active components adsorb more effectively onto the mild steel surface at higher concentrations, leading to enhanced protective film formation. Although surface coverage values were slightly lower at 60°C compared to 30°C, the extract still demonstrated significant adsorption capabilities under elevated temperature conditions.

3.6 Effect of Temperature

Temperature plays a significant role in understanding the mechanism of adsorption and corrosion inhibition efficiency. As shown in Table 5, increasing the temperature from 303 K to 333 K leads to a decrease in the adsorption equilibrium constant (K_{ads}) and a less negative Gibbs free energy of adsorption (∇G^0_{ads}) suggesting a reduction in the adsorption strength at higher temperatures. This trend indicates that the adsorption of the *Axonopus compressus* extract on the mild steel surface is predominantly physisorptive, as physical adsorption typically decreases with increasing temperature due to the weakening of intermolecular forces[17]. To further interpret the temperature effect, the Arrhenius equation will be employed:

$$logCR = \log A - \frac{E_a}{2.303RT} \qquad \text{..... (17)}$$

where CR is the corrosion rate, A is the pre-exponential factor, E_a is the activation energy, R is the gas constant, and T is the absolute temperature. A plot of log (CR) vs 1/T (with which multiplication by 1000 is usually done for graph plotting convenience) will provide the activation energy (E_a) from the slope;

$$(E_a = -slope \times 2.303R) \qquad \text{..... (18)}$$

This offers insights into the temperature sensitivity of the inhibition process. Generally, higher activation energy in the presence of an inhibitor implies a physical mode of adsorption, while lower activation energy may suggest a chemisorptive mechanism [17]. This approach complements the isotherm analysis and strengthens the understanding of the extract's inhibitory action under varying thermal conditions.

Table 5 The logarithm of Corrosion rate with reciprocal of absolute temperature $(\boldsymbol{K^{-1} \times 10^3})$

Sample	Conc. (g/ml)	CR (mmpy)		$logCR$		$\frac{1}{T}$ $(K^{-1} \times 10^3)$	
		30⁰C	60⁰C	30⁰C	60⁰C	30⁰C (303K)	60⁰C (333K)
Sample A	0	9.57	119.66	0.9809	2.0779	3.30	3.00
Sample E	0.4	4.1	61.54	0.6128	1.7892	3.30	3.00
Sample D	0.7	3.42	51.28	0.5340	1.7099	3.30	3.00
Sample B	2.1	2.73	41.02	0.4362	1.6130	3.30	3.00
Sample C	2.8	0.68	20.52	-0.1675	1.3122	3.30	3.00

The plot of log (CR) vs 1/T in Figure 6 shows that as temperature increases (1/T decreases), log (CR) rises, indicating a faster corrosion rate. This trend confirms that corrosion is thermally activated, becoming more aggressive at higher temperatures. It also suggests that the inhibitor's effectiveness weakens with heat, reinforcing a physisorption mechanism[17-19]. However, literature has suggested that corrosion behavior in CO_2environments is not strictly linear with temperature. At temperatures above 60°C and particularly approaching 90°C corrosion rates may begin to decline due to the formation of protective scales, predominantly composed of iron carbonate (F_eCO_3), which can act as a barrier to further metal degradation [20].

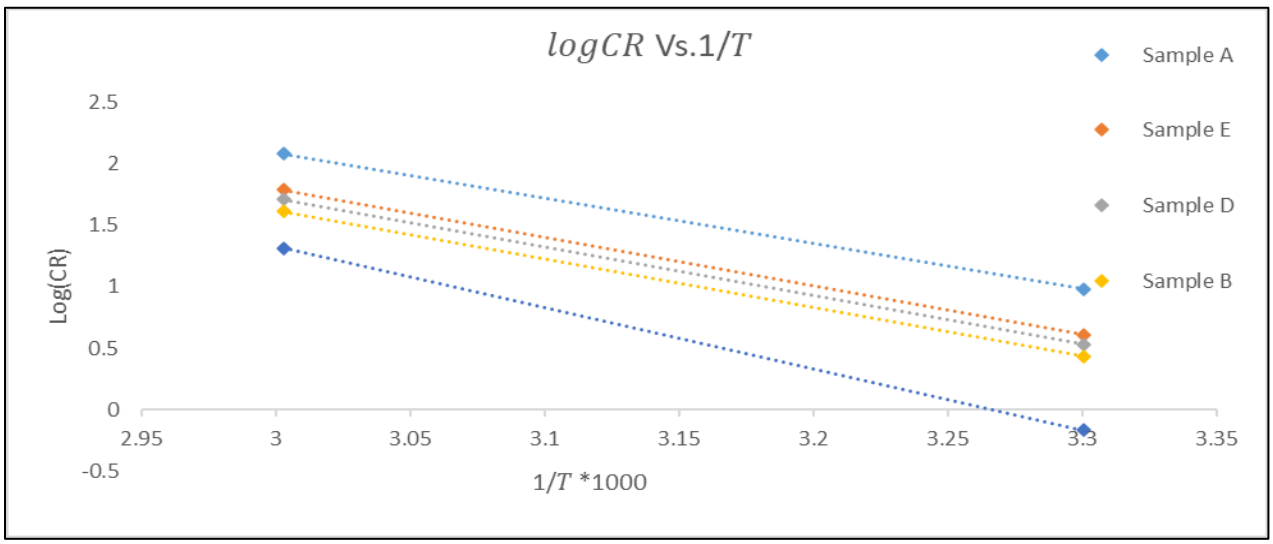

Figure 6 The relationship of logarithm of Corrosion rate with reciprocal of absolute temperature $(\boldsymbol{K^{-1} \times 10^3})$

3.7 Adsorption Isotherms

Adsorption isotherms involve conducting multiple adsorption measurements at a specific temperature and depicting the outcomes as a correlation between the quantities of adsorbed and non-adsorbed insights into the characteristics of the adsorption phenomenon. The commonly used isotherms, Langmuir and Freundlich are considered in this work. The adsorption isotherm is critical in estimating the standard adsorption Gibbs energy (∇G^0_{ads}) making use of the calculated inhibition efficiency at different inhibitor concentrations [21].

For Langmuir adsorption isotherm, the relationship between surface coverage and the extract concentration in the bulk solution is given by [21].;

$$K_c = \frac{\theta}{1-\theta} \quad \text{..... (19)}$$

Where k = adsorption equilibrium constant. Rearranging the equation,

$$\frac{c}{\theta} = \frac{1}{k} + C,\ C = \frac{1}{\theta_m} \quad \text{..... (20)}$$

To make it linear, it can be rearranged as follows:

$$\frac{1}{\theta} = \frac{c}{k\theta_m} + \frac{1}{\theta_m}, \quad \text{..... (21)}$$

where; θ_m = maximum adsorption capacity. c = equilibrium concentration of the adsorbate and k = equilibrium constant.

This equation has the form $y = mx + b$ ..... *(22)*

Where; $y = \frac{1}{\theta}$, $x = c$, $m = \frac{1}{k\theta_m}$ (the slope of the linear graph), and $b = \frac{1}{\theta_m}$ (y-intercept)

$$\nabla G^0_{ads} = -2.303RT\log(55.5K) \quad \text{..... (23)}$$

Where; ∇G^0_{ads} = Standard Adsorption Gibbs Energy, R = Gas constant, T= Temperature and k =

The linearized form of the Langmuir, Freundlich adsorption isotherm equation is given below;

Langmuir: $\frac{c}{\theta} = \frac{1}{k} + C,$ ..... *(24)*

Freundlich: $Log\theta = LogK + mLogC$ ..... *(25)*

From Table 6 and Table 7, the experimental data, shows the R^2, Slope, K_{ads}, and ∇G^0_{ads}

From the Figure7 – Figure 8, it can be seen that the Langmuir adsorption isotherm best explains the adsorption properties. The Langmuir plots presented in Figure 7 exhibit slopes close to unity and intercepts near zero, consistent with the ideal Langmuir adsorption behavior as described by [21]. Additionally, the coefficient of determination (R^2) for the Langmuir model is significantly higher at both 303 K (R^2 = 0.9562) and 333 K (R^2 = 0.9625), indicating a better fit compared to the Freundlich model, which shows notably lower R^2 values of 0.4042 and 0.3540 at the respective temperatures. This suggests that the Langmuir model provides a more accurate representation of the adsorption process of the plant extract onto the mild steel surface.

Table 6 The table shows the data for the Langmuir and Freundlich Adsorption Isotherms for Adsorption of Extract of *Axonopus compressus* onto the mild steel surface.

Conc. (C)	**(θ)**		**(C/θ)**		**LN (C)**		**LN(θ)**	
	30^{0}C	60^{0}C	30 ^{0}C	60 ^{0}C	30 ^{0}C	60 ^{0}C	30 ^{0}C	60 ^{0}C
0	0	0	0	0	0	0	0	0
0.4	0.57	0.49	0.7	0.82	-0.9163	-0.9163	-0.5621	-0.7133
0.7	0.64	0.57	1.09	1.23	-0.3567	-0.3567	-0.4463	-0.5621
2.1	0.71	0.66	2.96	3.18	0.7419	0.7419	-0.3425	-0.4155
2.8	0.93	0.83	3.01	3.37	1.0296	1.0296	-0.0726	-0.1863

Furthermore, the Gibbs free energy of adsorption (∇G^0_{ads}) values derived from the Langmuir model, as shown in Table 7, are in good agreement with those calculated using the conventional method. All ∇G^0_{ads} values are negative and fall below -20 kJ/mol, indicative of a spontaneous physisorption process[22-23]. The maximum adsorption capacity

increases with concentration, as reflected in Table 6, and the calculated C/θ values further support monolayer formation on a homogeneous surface, a hallmark of Langmuir-type adsorption.

These observations confirm the suitability of the Langmuir isotherm model in describing the adsorption behavior of *Axonopus compressus* extract on mild steel. While Langmuir adsorption is often associated with chemisorption, its versatility also extends to physisorption, particularly in systems where adsorption occurs as a uniform monolayer.

Table 7 The table shows the various Adsorption Isotherms for Adsorption of Extract of *Axonopus compressus* onto the mild steel surface at 163 hr.

Isotherm	**Temp.(K)**	**R^2**	**Slope**	**Intercept**	**K_{ads}**	**∇G^0_{ads} (KJ/mol)**
Langmuir	303	0.9562	1.1184	0.2099	4.76	-14.05
Freundlich	303	0.4042	0.1928	-0.3039	3.29	-13.12
Langmuir	333	0.9625	1.1290	0.4565	2.19	-12.09
Freundlich	333	0.3540	0.2141	-0.3968	2.52	-12.45

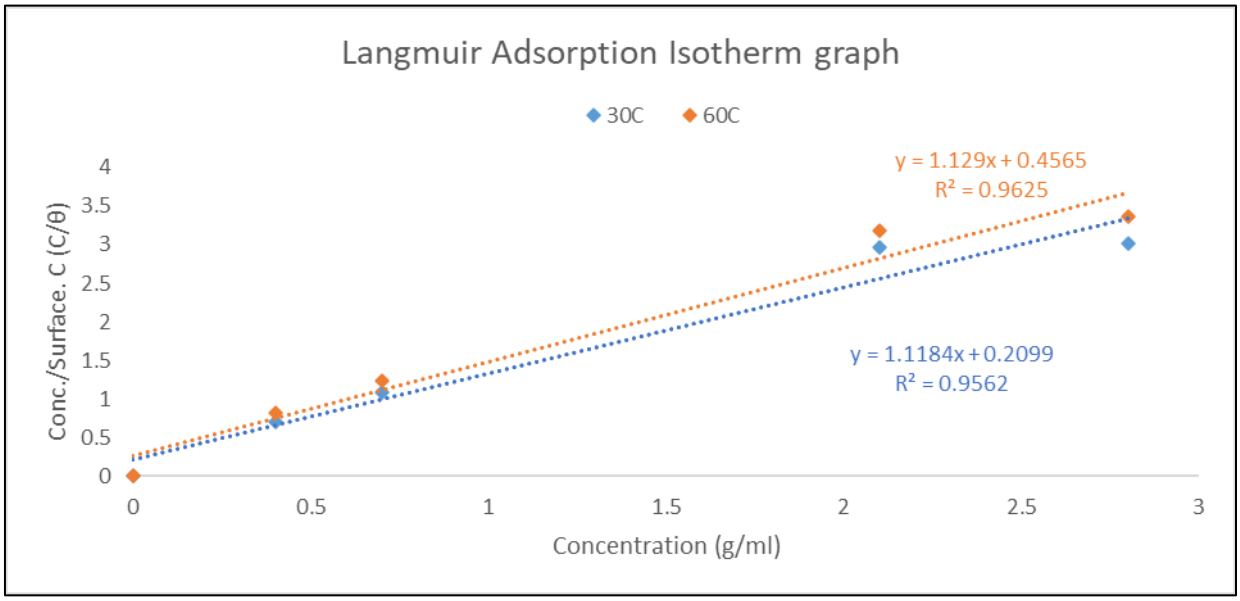

Figure 7 The Langmuir Adsorption Isotherm**.**

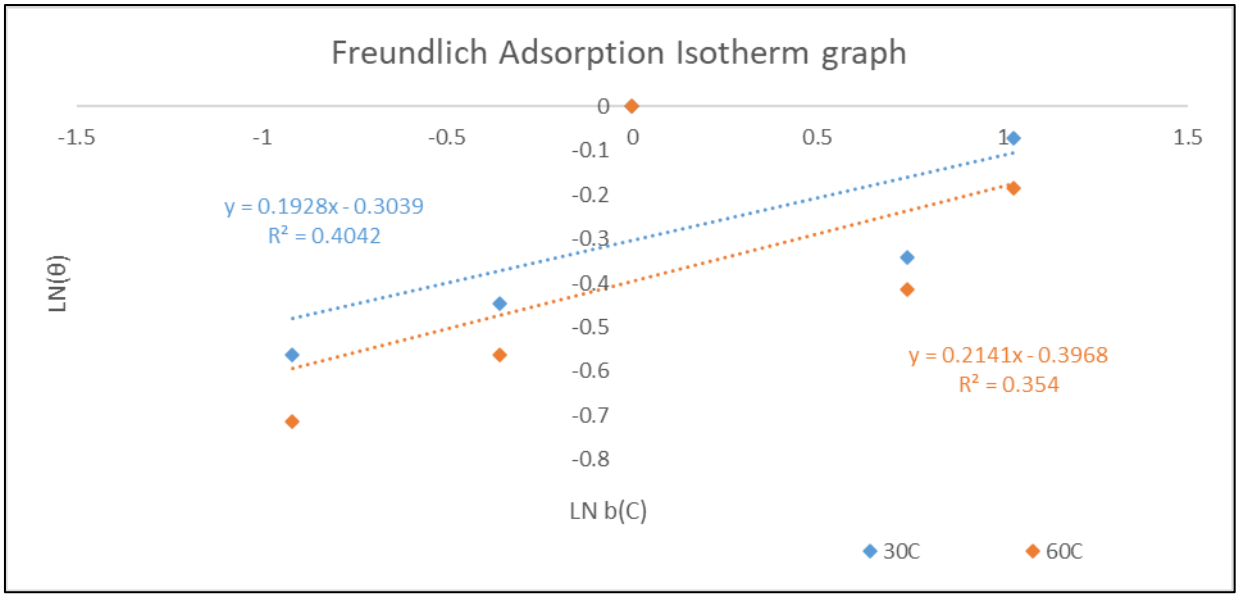

Figure 8 The Freundlich Adsorption Isotherm

4 Conclusion

This study has successfully demonstrated the potential of *Axonopus compressus* (carpet grass) extract as an effective and eco-friendly corrosion inhibitor for mild steel in a CO_2-saturated acidic environment. Weight loss and corrosion rate analyses revealed that the inhibition efficiency increased with higher concentrations of the extract, achieving optimal performance at 2.8 g/ml (40% w/w), where the corrosion rate dropped significantly. The temperature dependence of the inhibition process was evident, as higher temperatures led to increased corrosion rates and reduced inhibition efficiency, indicating a physisorption-dominated adsorption mechanism.

Adsorption isotherm modeling further confirmed the suitability of the Langmuir isotherm in describing the interaction between the inhibitor molecules and the metal surface, with high correlation coefficients ($R^2 > 0.95$) and ∇G^0_{ads} values indicating spontaneous physical adsorption. The Arrhenius plots supported these findings by showing that corrosion is thermally activated and that the extract increases the activation energy of the corrosion process, thereby impeding the rate of metal degradation.

Compliance with ethical standards

Disclosure of conflict of interest

The authors declare that they have no known competing financial interests or personal relationships that could have appeared to influence the work reported in this paper.

References

[1] Shehata OS, Korshed LA, Attia A. Green corrosion inhibitors, past, present, and future. Corrosion inhibitors, principles and recent applications. 2018 Apr 4:121.

[2] Goni LK, Mazumder MA. Green corrosion inhibitors. In Corrosion inhibitors 2019 Apr 30. IntechOpen.

[3] Eduok U, Szpunar J. Corrosion inhibitors for sweet oilfield environment (CO 2 corrosion). Corrosion Inhibitors in the Oil and Gas Industry. 2020 Apr 6:177-227.

[4] Aribo S, Olusegun SJ, Ibhadiyi LJ, Oyetunji A, Folorunso DO. Green inhibitors for corrosion protection in acidizing oilfield environment. Journal of the Association of Arab Universities for Basic and Applied Sciences. 2017 Oct 1;24:34-8.

[5] Elgaddafi R, andSubhash Shah RA. Research Article Modeling CO2-H2S Corrosion of Tubular at Elevated Pressure and Temperature. Research Journal of Applied Sciences, Engineering and Technology. 2016;13(7):510-24.

[6] Fazal BR, Becker T, Kinsella B, Lepkova K. A review of plant extracts as green corrosion inhibitors for CO2 corrosion of carbon steel. npj Materials Degradation. 2022 Jan 25;6(1):5.

[7] Usman BJ, Ali SA. Carbon dioxide corrosion inhibitors: a review. Arabian Journal for Science and Engineering. 2018 Jan; 43:1-22.

[8] Nešić S. Carbon dioxide corrosion of mild steel. Uhlig's corrosion handbook. 2011 Mar 1; 51:229-45.

[9] Remita E, Tribollet B, Sutter E, Vivier V, Ropital F, Kittel J. Hydrogen evolution in aqueous solutions containing dissolved CO2: Quantitative contribution of the buffering effect. Corrosion science. 2008 May 1;50(5):1433-40.

[10] Javidi M, Bekhrad S. Failure analysis of a wet gas pipeline due to localised CO2 corrosion. Engineering Failure Analysis. 2018 Jul 1; 89:46-56.

[11] Žbulj K, Hrnčević L, Bilić G, Simon K. Dandelion-root extract as green corrosion inhibitor for carbon steel in CO2-saturated brine solution. Energies. 2022 Apr 22;15(9):3074.

[12] Singh A, editor. Corrosion inhibitors. BoD–Books on Demand; 2019 Aug 7.

[13] Alrefaee SH, Rhee KY, Verma C, Quraishi MA, Ebenso EE. Challenges and advantages of using plant extract as inhibitors in modern corrosion inhibition systems: Recent advancements. Journal of Molecular Liquids. 2021 Jan 1; 321:114666.

[14] Sapunyo WL, Mbaria JM, Kanja LW, Omolo MJ, Onyancha JM. Phytochemical screening, toxic effects, and antimicrobial activity studies of Digitariaabyssinica (hochst. Ex A. Rich.) Stapf (Poaceae) Rhizome extracts against selected Uropathogenic microorganisms. Evidence-Based Complementary and Alternative Medicine. 2023;2023(1):4552095.

[15] Afolabi F, Afolabi OJ. Phytochemical constituents of some medicinal plants in South West Nigeria. IOSR J Appl Chem. 2013;4(1):76–78.

[16] Oguzie EE, Unaegbu C, Ogukwe CN, Okolue BN, Onuchukwu AI. Inhibition of mild steel corrosion in sulphuric acid using indigo dye and synergistic halide additives. Materials chemistry and physics. 2004 Apr 1;84(2-3):363-8.

[17] Abeng FE, Idim VD, Obono OE, Magu TO. Adsorption and adsorption isotherm: application to corrosion inhibition studies of mild steel in 2 M HCl. World Scientific News. 2017;77(2):298-313.

[18] Ebenso EE, Eddy NO, Odiongenyi AO. Corrosion inhibition and adsorption properties of methocarbamol on mild steel in acidic medium. PortugaliaeElectrochimica Acta. 2009 Feb 17;27(1):13-22.

[19] Ulaeto SB, Ekpe UJ, Chidiebere MA, Oguzie EE. Corrosion inhibition of mild steel in hydrochloric acid by acid extracts of Eichhornia crassipes. Int. J. Mater. Chem. 2012;2(4):158-69.

[20] Eškinja M, Moshtaghi M, Hönig S, Zehethofer G, Mori G. Investigation of the effects of temperature and exposure time on the corrosion behavior of a ferritic steel in CO2 environment using the optimized linear polarization resistance method. Results in Materials. 2022 Jun 1;14:100282.

[21] Kokalj A. On the use of the Langmuir and other adsorption isotherms in corrosion inhibition. Corrosion Science. 2023 Jun 1;217:111112.

[22] Mejeha IM, Uroh AA, Okeoma KB, Alozie GA. The inhibitive effect of Solanum melongena L. leaf extract on the corrosion of aluminium in tetraoxosulphate (VI) acid. African Journal of Pure and Applied Chemistry. 2010 Aug;4(8):158-65.

[23] Ikpi ME, Udoh II, Okafor PC, Ekpe UJ, Ebenso EE. Corrosion inhibition and adsorption behaviour of extracts from Piper guineensis on mild steel corrosion in acid media. International Journal of Electrochemical Science. 2012 Dec 1;7(12):12193-206.